NANO LETTERS

2001
Vol. 1, No. 4
169−174

Nanostructuring of Carbon Surfaces by Deposition of a Channel-Forming Protein and Subsequent Polymerization of Methyl Methacrylate Prepolymers

Michael Niederweis* and Christian Heinz

Lehrstuhl für Mikrobiologie, Friedrich-Alexander Universität Erlangen-Nürnberg, Staudtstrasse 5, 91058 Erlangen

Katharine Janik and Stefan H. Bossmann*

Lehrstuhl für Umweltmesstechnik, Universität Karlsruhe (TH), Engler-Bunte-Ring 1 76128 Karlsruhe

Received January 9, 2001 *(Revised Manuscript Received February 21, 2001)*

ABSTRACT

A novel procedure for nanostructuring on carbon surfaces by depositing buffer droplets containing a unique protein (MspA porin from *Mycobacterium smegmatis*) and a PMMA prepolymer, followed by thermal curing and high vacuum treatment, was developed. The formation of protein/PMMA nanostructures on carbon surfaces depended on the amount of protein/prepolymer deposited and the temperature during and after the deposition process. The nanostructures were analyzed quantitativly using computer-supported high-resolution transmission electron micrography (TEM).

Introduction. In the current literature, a wide range of methods for the nanostructuring of (mostly metal) surfaces is reported. The most advanced technologies are commonly described as electrochemical nanostructuring (by tip-induced metal deposition or oxidation)[1−3] and atomic force microscope (AFM) lithography.[4−6] Electrochemical methods are based on the technology of the scanning tunneling microscope (STM).[7−9] Finally, we must not neglect the lithography procedures with the highest application potential so far, namely photolithograhy,[10] electron-beam lithography,[11] and soft lithography.[12] However, until now the most significant disadvantage of electrochemical nanostructuring and AFM lithography is that nanostructuring has to be performed atom by atom or fragment by fragment, respectively. Consequently, the defined nanostructuring of surfaces has been time consuming and expensive. Therefore, the generation of well-defined nanostructures by protein or macromolecule deposition on two-dimensional surfaces would represent a considerable advantage compared to the technologies previously mentioned. In recent years, great progress has been made in the quantitative determination of the driving forces responsible for the formation of supramolecular structures in the electronic ground states[13−15] such as charge-interactions,[16] hydrogen bonding,[17] and hydrophobic forces.[18] This kind of analysis is not yet possible for the deposition of polymer- and protein-monolayers on surfaces. However, many well-ordered structures of proteins at surfaces have been obtained by using a variety of deposition techniques.[19−21] Nanostructured layers on surfaces possess many interesting electrochemical and photoelectrochemical properties[22] and have been used successfully for the design of electrochemical biosensors.[23,24] In addition, the formation and properties of self-assembled nanostructures made from proteins can be tailored to specific needs by site-directed mutagenesis. However, most proteins lose their structural integrity in a nonnative environment and therefore cannot be used in technical processes. The MspA porin from *M. smegmatis* is an extremely stable protein, which retains its channel structure even after boiling in 3% SDS or extraction with organic solvents.[25] Such a stable channel protein is an ideal template for synthesis of nanocompounds. We, therefore, have developed methods to obtain ordered nanostructures with MspA.

In this study, we show that the MspA porin forms distinct nanostructures on carbon surfaces when co-deposited together with PMMA prepolymers in the form of protein/buffer microdroplets. We consider our work as one of the first examples of a simple shape selective deposition procedure

* Corresponding authors. E-mail: mnieder@biologie.uni-erlangen.de; ie61@mv70.rz.uni-karlsruhe.de

10.1021/nl015503x CCC: $20.00
Published on Web 03/24/2001

of nanostructured surface elements, which can serve for many applications in the field of life sciences as well as for the stabilization of metal nanoparticles.

Materials and Methods. (1) General Information. The analysis of the two-dimensional nanostructures could be performed using AFM,[26] STM,[27] and TEM (transmission electron micrography).[28−30] Whereas AFM and especially STM permit an extremely well-resolved spatial resolution, TEM is the method of choice for the analysis of extended nanostructured surfaces.

The TEM images were recorded using a transmission electron micrograph EM 912/Zeiss equipped with an Omega filter system. In addition, an STI video camera was employed. The scanning of the samples, prior to the measurements, was performed using a low electron dose of approximately $6.5 \pm 0.5 \times 10^4$ electrons s^{-1} nm^{-2}. Electron-induced polymerization was achieved using electron doses of $1.25 \pm 0.55 \times 10^5$ electrons s^{-1} nm^{-2}. After the polymerization processes were completed, the nanopatterned surfaces appeared to be stable when analyzed using the latter electron dose.

For the analysis of the TEM images, the IMAGE-software, generously provided by the National Institutes of Health (NIH), was used.[31] Commercially available PAMAM starburst dendrimers (Michigan Molecular Institute) possessing distinct diameters and masses were deposited on identical carbon surfaces and used for the calibration of the IMAGE software.

(2) Purification of the MspA Porin. *Mycobacterium smegmatis* was grown using published procedures.[32]

(3) Photopolymerization of Methyl Methacrylate and Formation of PMMA Prepolymers. Photopolymerization of MMA (Aldrich) was performed in an annular Pyrex-photoreactor (length, 13 cm; diameter, 5 cm; irradiated layer, 0.5 cm) equipped with a mercury medium-pressure arc (Heraeus TQ 150) and a water cooling system ($T = 18.2$ °C). Irgacure (1.0×10^{-3} M (Aldrich)) was used as the photoinitiator. The PMMA/MMA prepolymer employed in our experiments contained a macromolecular fraction ($11.5 \pm 0.25\%$) of PMMA ($M_n = 37.400$; $P_d = 5.2$).

(4) Surface Patterning/TEM Sample Preparation. The standard sample was prepared by dispersing 0.50 mL of a 1.0 μg/mL of MspA and 1.25 μg/mL of PMMA/MMA prepolymer containing PS01 buffer solution using a sonication system (PTS 250W, Siemens). In general, when sonication is used, there is always the danger of bond disruption, followed by the decay of the materials to be disposed. We have demonstrated using the well-known PAMAM starburst dendrimer (SBD G 4.5, see below) that sonication under exactly the same conditions as during deposition, but for 500 s instead of typically 125 s, does not lead to any decomposition! Therefore we consider our deposition method safe. (See Figure S2 in the Supporting Information).

The microdroplets were deposited on a special TEM surface (available from Plano/Marburg, total surface area: 1.0 cm^2) consisting of a copper net (distance of the copper wires: 85 μm), which is laminated with polyvinylformaldehyde (PVF; thickness: 20−40 nm). The PVF was sputtered using elemental carbon. This particular surface was exposed to the protein/buffer microdroplets for 125 s, unless otherwise noted (distance from the buffer-surface: 5.0 cm). After the initial deposition, the protein buffer film was allowed to equilibrate for 30 min at defined temperatures. Finally, most of the water was removed in high vacuum over 24 h.

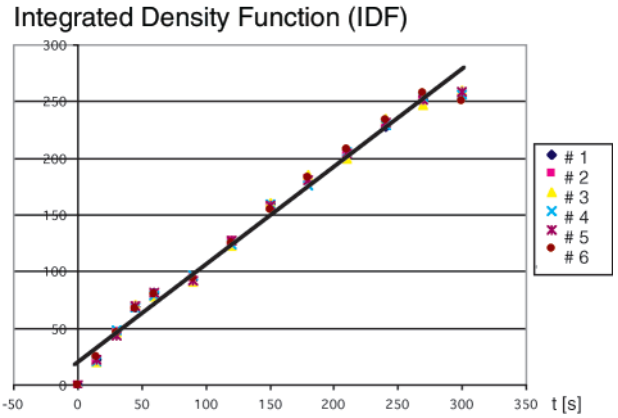

Figure 1. Plot of the IDF values (calculated by using IMAGE) vs the sonication time of the SBD G 4.5 solution ($c = 2.25$ μg/mL) in PS01 buffer concentration. A linear dependency was observed ($R = 0.9912$) up to the formation of a SBD G 4.5 monolayer (IDF = 255) at the carbon surface. These six experiments were all made independently of each other.

(5) Computer-Assisted Analysis of the P(MMA/DPB) Morphology and Calibration Procedure. The analysis of all available TEM images (10−20 per experiment) was performed by the computer program IMAGE. Surface plots of the (nano)structures investigated are presented together with the original TEM images. A quantitative analysis of the nanoscopic structures, generated by deposition of protein and prepolymer containing buffer droplets at the carbon surface, was achieved by depositing SBD G 4.5 (diameter: 8.79×10^{-9} m, molecular weight: 19661 g mol^{-1}, surface area: 2.433×10^{-26} m^2)[33] on the TEM surface using exactly the same buffer composition and deposition procedure except that MspA and PMMA/MMA were substituted by SBD G 4.5. The concentration of SBD G. 4.5 in PS01 buffer was 2.25 μg/mL.

Next, 0.50 mL of the SBD G 4.5 solution was dispersed by sonication during 15 to 300 s. The integrated density function (IDF) of the software IMAGE permits the calibration of the thickness of the deposited layer. Areas of 100 nm × 100 nm were integrated and the corresponding IDF values summarized in Figure 1. An IDF value of 255 corresponds to a formed monolayer of SBD G 4.5 at the carbon surface (see also the Supporting Information). A monolayer of SBD G 4.5 at the carbon surface, which was formed after 250 s of deposition, corresponds to a deposited mass of 1.35×10^{-8} g/cm^2. As it becomes clear from Figure 1, a linear deposition of SBD G 4.5 occurs up to a sonication time of 250 s.

Results and Discussion. This research endeavor consists of the development of a straightforward experimental procedure that permits lateral (nano)structuring at suitable

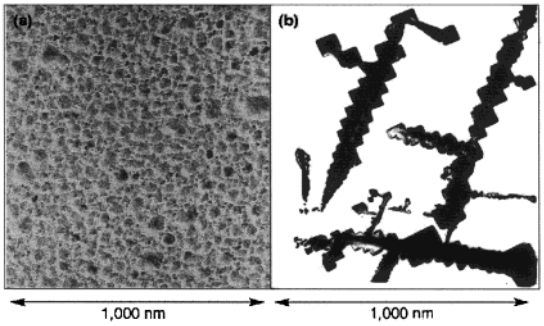

Figure 2. Effect of the deposition of P(MMA)/buffer (c = 2.25 g/mL) (a) in comparison to MspA/P(MMA)/buffer (c(MspA) = 1.00 g/mL, (c(PMMA/MMA) = 1.25 g/mL)) (b) at carbon surfaces (TEM image).

surfaces. We used the MspA protein because of its superior stability[32] compared with other classes of proteins isolated from bacteria. MspA porin was selectively extracted from whole cells of *M. smegmatis* and purified by anion exchange and gel filtration chromatography as described recently.[32] The SDS−polyacrylamide gel shows that MspA was purified to apparent homogeneity (Figure S1, lane 2). Lipid bilayer experiments demonstrated that this MspA preparation had high channel-forming activity (data not shown). In a separate study, the MspA protein demonstrated its ability to form a wide range of nanostructures, including a nanochannel containing phase at a carbon surface.[34] However, the nanostructured MspA phases redissolved easily in various aqueous buffers. This effect clearly hampers any future application. Therefore, we attempted to stabilize formed nanochannels using P(MMA). It could be expected that the phases formed using MspA and P(MMA) differ to various extents from the phases where MspA was used alone. Because only very little is known to this date about the prospect of self-structuring protein/polymer phases, the results are of great interest with respect to the generation of distinct shapes in the submicro and nanoscale.

In Figure 2, the effect of the presence of MspA during the buffer deposition from the gas phase onto a carbon surface becomes clear. Without the presence of MspA, only disordered structures of P(MMA) (pre)polymers can be found, whereas distinct and reproducible (nano)structures are formed if MspA is present. This finding provides the first evidence for the importance of MspA for the generation of ordered structures at surfaces.

To reach the goal of generating defined (nano)structures at a carbon surface, the general deposition procedure of the MspA/P(MMA) buffer (PS01) was varied to explore its possibilities. Note that this procedure using buffer sonication and the following deposition of microdroplets at the carbon surface differs from a conventional adsorption procedure, because no equilibrium exists between MspA/P(MMA) and the surfaces. Therefore, the exposition time of the surface toward the PS01 buffer is the decisive factor for the amount of MspA/P(MMA) deposited. A second very important experimental factor is the deposition temperature. The systematic variation of the sonication times (50, 75, 100, 125, 150, 175, and 200 s) and the temperature during deposition (20 °C, 25 °C, 30 °C, 35 °C, 40 °C) led to the discovery of two distinct deposition conditions, *with remarkable and reproducible patterns*.

(1) Formation of Microletters. When a depositon time of 125 ± 5 s and a deposition temperature of 30 ± 2 °C is chosen, the formation of "microletters" is observed. Typical "letters" are shown in Figure 3. This particular occurrence (thickness > 100 nm) is typical for a deposited pattern that was only investigated by TEM for a short time (less than 60 s).

(2) Formation of Dendrites and Stars. In Figure 4, dendrites and "stars" generated by deposition of MspA for 175 ± 5 s at 40 ± 5 °C at the chosen carbon surface are shown. The comparison of the occurrence of this micropattern at very low TEM exposition times (t < 60s) and after 300 s of electron beam treatment reveals polymerization of MMA included in the formed micropattern. The average thickness of the formed dendrites and stars was approximately 110 to 120 nm in the beginning of the TEM characterization, whereas the thickness decreased to 25 to 30 nm after 300 s of continuous electron beam exposure. In addition to the observed polymerization process, evaporation of water and MMA molecules into the high vacuum can be detected. Consequently, the diameter of the TEM beam of approximately 3000 nm can be seen in Figure 4 (300 s). However, this behavior is typical for all micropatterns investigated in this study. In all cases, the geometries initially formed during MspA deposition are retained during the electron beam treatment. This finding makes this simple deposition process of particular interest for the lateral nanostructuring of surfaces.

(3) Electron Beam Induced Polymerization of MMA

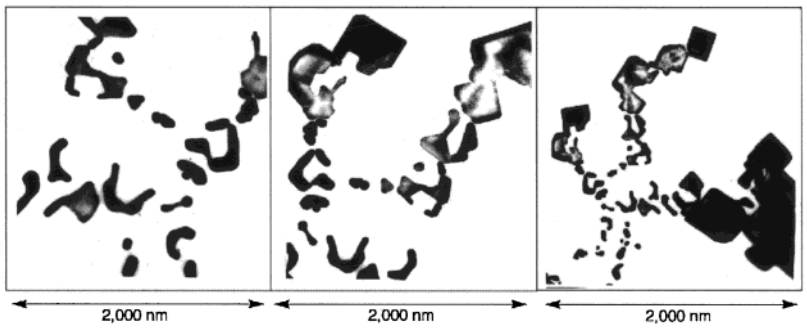

Figure 3. Microletters formed by deposition of MspA/P(MMA)/buffer at the carbon surfaces (TEM image, three different deposition experiments).

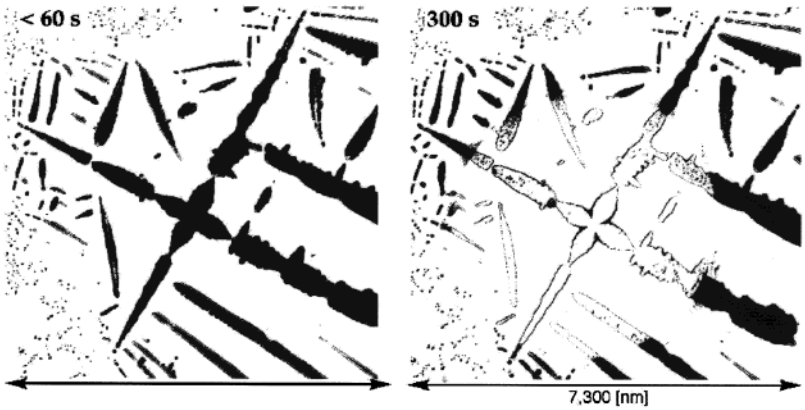

Figure 4. Dendrites and stars formed by deposition of MspA/P(MMA)/buffer at the carbon surface (TEM image) after < 60 and 300 s exposure to the electron beam.

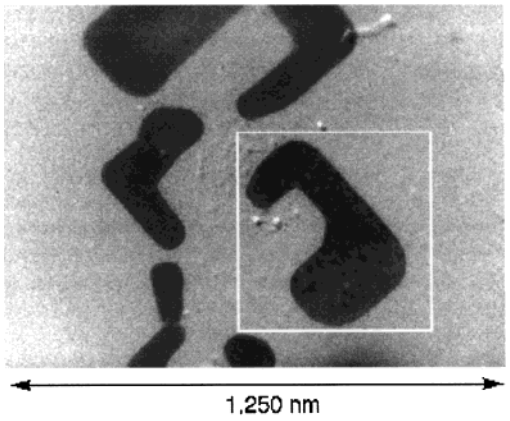

Figure 5. A typical microletter formed by deposition of MspA/P(MMA)/buffer at the carbon surface (TEM image). The impact of electron beam treatment leading to MMA polymerization of the letter within the white square will be summarized in Figure 6a.

in Microletters and Quantitative Analysis of the Micropattern by Using IMAGE. In Figure 5, a typical microletter is marked by a white square. The impact of the electron beam of the TEM on this microletter will be discussed in detail using both high-resolution TEM images and the program package IMAGE, which permits the calculation of the MspA/P(MMA) surface topologies using the TEM images as input.

Figure 6a presents a series of images of the microletter marked in Figure 5, which was treated continuously by the TEM electron beam. Whereas the letter appears to be relatively homogeneous at the beginning of the electron beam fixation process, a patchwork of black and gray spots is present after 120 and 240 s. However, after 300 s the interior of the microletter becomes homogeneously gray and a sharp edge remains, which represent the exact geometric shape of the letter immediately after its deposition on the carbon surface. The analysis of the TEM images using the program package IMAGE and using the calibration parameters obtained by the deposition of SBD G 4.5 (see Experimental section) reveals striking insights into this fixation process, which are summarized in Figure 6b. In the beginning of the electron beam exposure, the inner region of the microletter structure is smooth and possesses a thickness of 100−120 nm. In the course of the progressing reaction, holes with a diameter of 2−5 nm appear randomly distributed throughout the entire interior of the microletters. On the bottom of these holes exists an organic layer of a thickness of approximately 25 nm. In conclusion, the depth of the formed holes is approximately 75−95 nm. These hole regions grow consequently until most of the interior consists of an organic layer of 20−25 nm thickness. The surface of this layer structure is obviously rough.

A strong possibility exists that channel-like structures possessing a diameter of approximately 1−2 nm are randomly oriented within this layer. From our IMAGE analysis, it appears that holes, cavities, and/or channels exist at particular locations, where organic material is missing. However, using TEM we could not elucidate whether channels exist that are open to the surface of the microstructure. According to the IMAGE calibration procedure, the mass deposited in the interior of the microletters is approximately 2.7×10^{-9} g/cm^2.

In contrast to the interior of the microletters, their border regions form a wall-type structure, which is not affected by the continuous electron beam exposure. The diameter of these walls is approximately 65 nm at the bottom. The deposited mass at the wall regions is considerably higher (2.1×10^{-8} g/cm^2) than in the interior. After 300 s, only minor changes occurred in the fixed microletters at the carbon surface.

A detailed discussion of the electron beam induced polymerization of MMA in "stars" and the quantitative analysis of the formed micropattern is provided as Supporting Information.

(4) Mechanistic Hypothesis. In Figure 7, an enlargement of the final stages of both the microletter and the star phase is shown. We already pointed out that remarkable changes occur in the interior of the primarily deposited microstructures, whereas the wall-like structure at the boundary remains almost unchanged during continuous electron beam exposure.

On the basis of the experimental evidence available to date, we developed the following mechanistic hypothesis: The wall regions, which form the boundaries of the microstructure, might be formed from MspA and PMMA, which form hydrophobic aggregates. The chemical composition of these aggregates differs depending on the deposition conditions, such as MspA and PMMA concentrations and temperature.

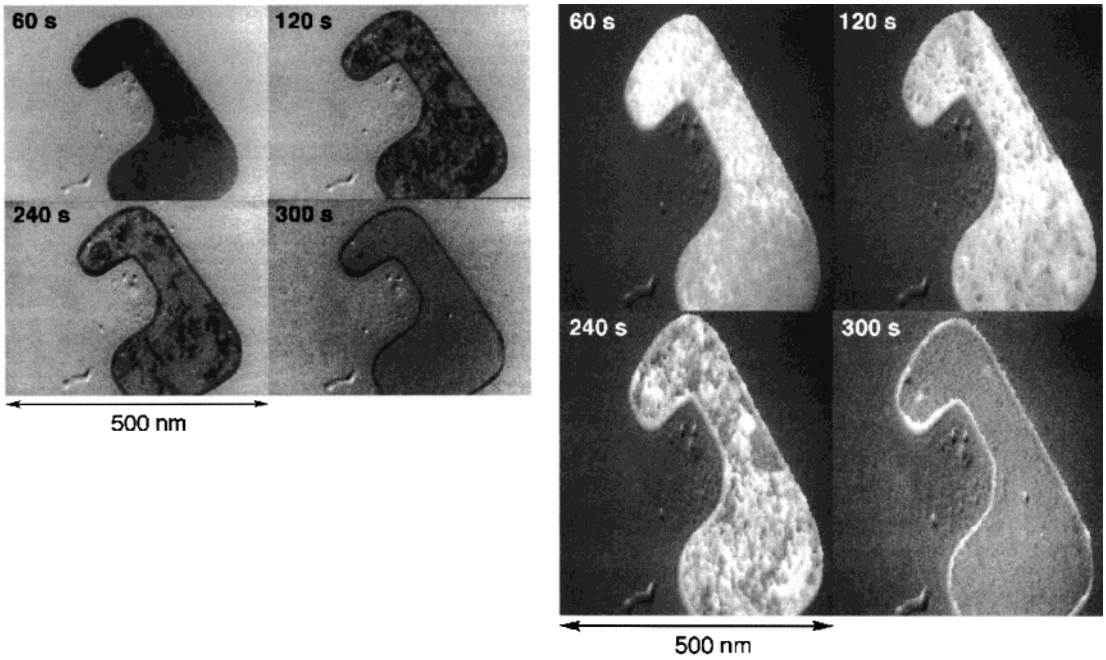

Figure 6. (a) TEM images of a typical microletter formed by deposition of MspA/P(MMA)/buffer at the carbon surface at various electron beam exposure times. (b) Surface plots of a typical microletter formed by deposition of MspA/P(MMA)/buffer at the carbon surface, calculated by IMAGE using the TEM images as input.

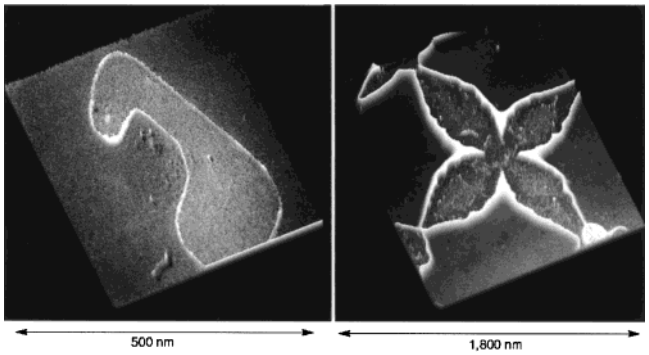

Figure 7. Enlarged surface plots of the final structures formed by MspA/P(MMA) at a carbon surface.

Neither the deposition of MspA nor PMMA prepolymers alone at the reported experimental conditions resulted in the formation of the microstructures reported here. Since PMMA is highly polydisperse ($P_d = 5.2$), it cannot be responsible for the patterning process. A control experiment supports this hypothesis (see Figure 2 and Figure S3). Therefore, it is very likely that both MspA and PMMA are the main building components of the wall-type structures: hydrophobic aggregates of MspA and PMMA develop during the deposition of the PS01 buffer microdroplets on the carbon surface. The hydrophobicity of the carbon surface itself may support the formation of these hydrophobic aggregates. Within the formed microstructures, hydrophilic cavities containing mostly MspA in aqueous buffer and a hydrophobic microphase consisting mostly of MMA and polymerization initiator coexist. H. M. McConnell and co-workers succeeded in the mathematical modeling of complex two-dimensional patterns in mixed surfactant bilayers, and also in protein layers, by using a line tension−dipole repulsions model.[35] The observed equilibrium shape of a constant-area monolayer was explained from the competition between the line tension of the domain boundary and the dipole−dipole repulsions between the molecular dipoles. Unfortunately, our much more complex and three-dimensional nanostructures cannot be explained as of yet by applying this model. However, we envision the mechanisms that lead to the formation of the distinct pattern during deposition to be very similar to those developed by McConnell in the two-dimensional phase.

Upon electron beam exposure and consequent heating of the microstructures, water and some of the MMA monomer evaporate in the high vacuum. The electron beam impact, as well as the increased temperature caused by TEM, leads to either anionic or radical MMA polymerization.[36] The gel effect is well known during MMA polymerization: at enhanced temperature the reaction rate of PMMA formation increases rapidly until a gel is formed from PMMA and the nonreacted MMA.[37] The formation of the gel results in a drastic *decrease* of the polymer volume.

Both the occurrence of the gel effect and the evaporation of H_2O or MMA at the same time may explain the appearance of holes during electron-beam impact. This process continues until neither H_2O nor MMA remains in the interior of the microstructures. Upon further observation it was evident that the wall regions do not exhibit the shrinking effect during electron beam impact, therefore we can conclude that only very little free H_2O and/or MMA is present in these regions after deposition.

Conclusion. Our experiments indicate a straightforward and dependable procedure for the generation of lateral nanostructures. The deposition of aerosol droplets generated by sonication of a buffer solution containing the MspA protein and a PMMA/MMA prepolymer onto a carbon

surface led to the reproducible formation of different types of structures. The presence of MspA can be regarded as the key factor for these remarkable formation processes. Dependable and inexpensive methods for the nanostructuring of two-dimensional surfaces will be the key to novel advanced technologies of the next millennium such as RAM chips of highest data storage capacity[38] and nanodiodes[39] for the development of superfast computers, or nanosensor arrays for the analysis of messenger substances in living cells.[40,41]

Acknowledgment. The authors thank Prof. Dr. D. Gerthsen and Mr. M. Fotouhi Ardakani for the recording of the TEM spectra. Financial support from the DFG and the Research Foundation of Baden-Württemberg is gratefully acknowledged.

References

(1) Fujita, D. *Nanotechnology* **1997**, *8*, 10.
(2) Reetz, M. T.; Helbig, W.; Quaiser, S. A.; Stimming, U.; Breuer, N.; Vogel, R. *Science* **1995**, *267*, 367−368.
(3) Hartmann, E.; Radojkovic, P.; Schwartzkopff, M.; Enachescu, M.; Marquardt, P. *Appl. Surf. Sci.* **1997**, *107*, 212−217.
(4) Blanckenhagen, P. v.; Gruber, A.; Gspann, J. *Nucl. Instrum. Methods Phys. Res., B* **1997**, *122*, 322−324.
(5) Held, R.; Vancura, T.; Heinzel, T.; Ensslin, K.; Holland, M.; Wegscheider, W. *Appl. Phys. Lett.* **1998**, *73*, 262−264.
(6) Craciun, F.; Verardi, P.; Dinescu, M.; Dinelli, F.; Kolosov, O. *Thin Solid Films* **1999**, *336*, 281−285.
(7) Heusler, K. E.; Budevski, E.; Staikov, G.; Lorenz, W. J. *Angew. Chem., Int. Ed. Engl.* **1997**, *36*, 1220.
(8) Kuznetsov, A. M.; Lorenz, W. *Chem. Phys.* **1997**, *214*, 243−252.
(9) Pötzschke, R. T.; Staikov, G.; Lorenz, W. J.; Wiesbeck, W. *J. Electrochem. Soc.* **1999**, *146*, 141−149.
(10) Wagner, C.; Kaiser, W.; Mulkens, J.; Flagello, D. G. *Solid State Technol.* **2000**, *43*, 97−108.
(11) Seebohm, G.; Craighead, H. G. *Electron Mater. Ser.* **2000**, *6 (Quantum Semiconductor Devices and Technologies)*, 97−138.
(12) Kane, R. S.; Takayama, S.; Ostuni, E.; Ingber, D. E.; Whitesides, G. M. *Biomaterials* **1999**, *20*, 2363−2376.
(13) Eblinger, F.; Schneider, H.-J. *Angew. Chem., Int. Ed. Engl.* **1998**, *37*, 7, 826−828.
(14) Schneider, H.-J.; Eblinger, F.; Sartorius, J.; Rammo, J. *J. Mol. Recognit.* **1996**, *9*, 123−132.
(15) Laitenberger, P.; Claessens, C. G.; Kuipers, L.; Raymo, F. M.; Palmer, R. E.; Stoddart, J. F. *Chem. Phys. Lett.* **1997**, *279*, 209−214.
(16) Kimizuka, N.; Kawasaki, T.; Hirata, K.; Kunitake, T. *J. Am. Chem. Soc.* **1998**, *120*, 4094−4104.
(17) Hansch, C.; Leo, A.; Hoekman, D. *J. Am. Chem. Soc.* **1996**, *118*, 8, 10678−10688.
(18) Lüdemann, S.; Abseher, R.; Schreiber, H.; Steinhauser, O. *J. Am. Chem. Soc.* **1997**, *119*, 4206−4213.
(19) Edmiston, P. L.; Lee, J. E.; Cheng, S.-S.; Saavedra, S. S. *J. Am. Chem. Soc.* **1997**, *119*, 560−570.
(20) Wood, L. L.; Cheng, S.-S.; Edmiston, P. L.; Saavedra, S. S. *J. Am. Chem. Soc.* **1997**, *119*, 571−576.
(21) Jeurnink, T.; Verheul, M.; Stuart, M. C.; Kruif, C. G. d. *Colloids Surf., B* **1996**, *6*, 291−308.
(22) Lahav, M.; Heleg-Shabtai, V.; Wasserman, J.; Katz, E.; Willer, I.; Dürr, H.; Hu, Y.-Z.; Bossmann, S. *J. Am. Chem. Soc.* **2000**, *122*, 11480−11487.
(23) Rusling, J. F. *Progr. Colloid Polymer Sci.* **1997**, *103*, 170−180.
(24) Hayes, W. A.; Shannon, C. *Langmuir* **1998**, *14*, 1099−1102.
(25) Niederweis, M.; Ehrt, S.; Heinz, C.; Klöcker, U.; Karosi, S.; Swiderek, K. M.; Riley, L. W.; Benz, R. *Mol. Microbiol.* **1999**, *33*, 933−945.
(26) Kaiser, S.; Preis, H.; Gebhardt, W.; Ambacher, O.; Angerer, H.; Stutzmann, M.; Rosenauer, A.; Gerthsen, D. *Jpn. J. Appl. Phys., Part 1* **1998**, *37*, 84−89.
(27) Heinz, R.; Stabel, A.; Rabe, J. P.; Wegner, G.; Schryver, F. C. D.; Corens, D.; Dehaen, W.; Süling, C. *Angew. Chem., Int. Ed. Engl.* **1994**, *33*, 3, 2080−2082.
(28) Tillmann, K.; Thust, A.; Lentzen, M.; Swiatek, P.; Förster, A.; Urban, K.; Laufs, W.; Gerthsen, D.; Remmele, T.; Rosenauer, A. *Philos. Mag. Lett.* **1996**, *74*, 309−316.
(29) Rosenauer, A.; Remmele, T.; Gerthsen, D.; Tillmann, K.; Förster, A. *Optik* **1997**, *105*, 99−107.
(30) Kaiser, S.; Preis, H.; Gebhardt, W.; Ambacher, O.; Angerer, H.; Stutzmann, M.; Rosenauer, A.; Gerthsen, D. *Jpn. J. Appl. Phys., Part 1* **1998**, *37*, 84−89.
(31) http://www.nih.gov
(32) Niederweis, M.; Ehrt, S.; Heinz, C.; Klöcker, U.; Karosi, S.; Swiderek, K. M.; Riley, L. W.; Benz, R. *Mol. Microbiol.* **1999**, *33*, 933−945
(33) Ben-Avraham, D.; Schulman, L. S.; Bossmann, S. H.; Turro, C.; Turro, N. J. *J. Phys. Chem. B* **1998**, *102*, 5088−5093.
(34) Niederweis, M., Bossmann, S.; international patent application (PCT/DE/02924).
(35) Perkovic, S.; McConnell, H. M. *J. Phys. Chem. B.* **1997**, *101*, 381−388.
(36) Echte, A. *Handbuch der Technischen Polymerchemie*; VCH: Weinheim, New York, 1993; pp 279−295.
(37) Reichert, K. H.; Moritz, H. U. Polymer Reaction Engineering. In Allen, Sir. G., Bevington, J. C. *Comprehensive Polymer Science*; Pergamon Press: Oxford 1989; p 334.
(38) Maoz, R.; Cohen, S. R.; Sagiv, J. *Adv. Mater. Including CVD - Chemical Vapor Deposition* **1999**, *11*, 55−60.
(39) Berger, S.; Schächter, L.; Tamir, S. *Nanostruct. Mater.* **1997**, *8*, 231.
(40) Kossek, S.; Padeste, C.; Tiefenauer, L. *J. Mol. Recognit.* **1996**, *9*, 485−487.
(41) Topoglidis, E.; Cass, A. E. G.; Gilardi, G.; Sheila Sadeghi; Beaumont, N.; Durrant, J. R. *Anal. Chem.* **1998**, *70*, 5111−5113.

NL015503X